Rev. Roum. Sci. Techn.– Électrotechn. et Énerg.
Vol. **70**, *3*, pp. 325–330, Bucarest, 2025

DYNAMIC BEHAVIOR ANALYSIS OF LOAD FREQUENCY CONTROL IN POWER SYSTEMS WITH HYBRID POWER PLANTS

GHAZANFAR SHAHGHOLIAN[1,2]

Keywords: Interconnected power system; Steam power plant; Gas power plant; Hydro power plant; Load frequency control.

In power systems, maintaining a nearly constant frequency is essential for stable operation. The secondary control loop plays a crucial role in regulating the system frequency, ensuring it remains at or near its nominal value. Additionally, this control loop is responsible for maintaining the scheduled power exchange between interconnected control areas via tie lines. This study focuses on analyzing and simulating the dynamic response of interconnected power systems under various configurations. The examined power system areas include steam, hydroelectric, and gas power plants. MATLAB-based simulations are conducted on both two-area and three-area power system models. The time-domain simulation results are further evaluated through eigenvalue analysis of the system matrix under different operating conditions. The findings indicate that, following a step change in load demand within isolated areas, gas power plants exhibit the smallest frequency deviation (droop). In contrast, hydroelectric plants demonstrate the largest frequency droop. Additionally, gas power plants exhibit fewer changes in response to load changes compared to the other two types of generation sources.

1. INTRODUCTION

Among various energy forms, electrical energy stands out as a pivotal element underpinning the growth of industrial, economic, and social sectors. Electricity generation is achieved through multiple types of power plants and technologies, which are primarily categorized by their primary energy source. Conventional thermal power plants, which rely on non-renewable energy sources, include steam power plants, gas-fired power plants, combined cycle plants, nuclear power plants, and diesel power plants. In contrast, renewable energy power plants encompass facilities that utilize various power sources, including hydroelectric, wind, geothermal, tidal, and solar energy. Typically, these power plants use one or more turbines coupled with generators to convert mechanical energy into electrical energy [3-9].

In the realm of power system control and stability, numerous persistent challenges arise, including unpredictable external disturbances, parameter uncertainties, and inaccuracies in the system modeling. These factors complicate achieving the desired operational performance. To address these issues, multiple control loops are implemented to regulate system parameters effectively, thereby ensuring stable and reliable operation of the power system. The problem of frequency deviation is an inherent and ongoing challenge that arises due to continuous fluctuations in load demand. Consequently, it necessitates adjustments in the generated power output to maintain the system frequency at its nominal setpoint [10-13]. In power systems, the load frequency control loop plays a critical role in maintaining the system frequency at its nominal value. The primary function of this control loop is to ensure that the active power output from generation units adequately meets the varying load demands.

Additionally, it regulates the power exchanged between interconnected control areas to keep it aligned with predetermined scheduled values, thereby maintaining system stability and operational reliability. The primary objective of the secondary control loop is to mitigate transient deviations in both area frequency and tie-line power exchange, while ensuring zero steady-state error in these parameters. Furthermore, this control loop enhances the overall stability of the power system [14,15]. Numerous studies have been conducted focusing on the design and enhancement of load frequency control stability within interconnected power networks [16,17].

A complementary control strategy is employed within the automatic generation control system to address the area control error. This approach adapts the controller gain using the integral square error criterion to enhance system performance. Additionally, in [18], a model predictive control method is proposed for a two-area interconnected power system that incorporates both photovoltaic and thermal generation units, providing a practical approach to load frequency control. When a discrete-time state-space model represents the dynamic characteristics of the system, the cost function used to optimize the control signal aims to minimize a weighted sum of the squares of the predicted errors and the squares of the future control actions. This approach ensures effective minimization of both tracking errors and control effort. With the rapid increase in photovoltaic penetration and integration into distributed grids, interconnected multi-area power systems are increasingly susceptible to disturbances. Such disturbances may originate from factors such as the parameters of grid-connected inverters, which can lead to amplified frequency fluctuations within the power system. In [19], a load frequency control approach utilizing double equivalent-input-disturbance controllers is introduced. This strategy is implemented using a linear model of the multi-area power system. The effectiveness of the proposed method in damping frequency fluctuations is demonstrated through simulation results.

Wind power plants play a significant role in supplying environmentally sustainable energy. However, their integration into power systems introduces stability challenges, primarily due to the inherent lack of inertia in wind-based generation. The stochastic nature of wind energy further contributes to potential disturbances in the power injected into the grid. In [20], the design and implementation of an optimal automatic generation control system based on a PI structure and utilizing full-state vector feedback control theory are presented for a two-area multi-source power system incorporating wind power plants. Simulation results indicate that wind power plants can amplify load disturbances when wind power availability decreases, yet this effect is counterbalanced when wind energy input increases, effectively mitigating the impact of load disturbances. Renewable energy sources are crucial for

[1] Department of Electrical Engineering, Na. C., Islamic Azad University, Najafabad, Iran.
[2] Smart Microgrid Research Center, Na. C., Islamic Azad University, Najafabad, Iran, E-mail: shahgholian@iau.ac.ir

DOI: 10.59277/RRST-EE.2025.70.3.7

electricity generation as they help reduce environmental pollution and decrease reliance on non-renewable resources. However, the integration of renewable energy introduces instability into the system's frequency response, and these fluctuations can degrade power quality. In [21], a linear active disturbance rejection control strategy based on the soft actor-critic approach is proposed to mitigate the negative impacts associated with renewable energy integration. This intelligent controller is subsequently applied to manage load frequency in a two-area interconnected power system. Simulation results demonstrate that the proposed control method outperforms several alternative approaches in terms of effectiveness. The growing integration of renewable energy sources into power systems has led to reduced system inertia, which is now recognized as a critical challenge.

This paper conducts a time-domain analysis and simulation of the dynamic behavior of the load frequency control system within an interconnected power network. Simulations are performed for a multi-area system comprising diverse combinations of steam, gas, and hydroelectric power plants. The dynamic characteristics are examined through eigenvalue analysis of the system matrix. The main objectives of this study are as follows:

- Comparison of dynamic responses: Evaluation and comparison of the dynamic behavior among different types of power plants.
- Analysis of system modes: Investigation of the system modes present in interconnected power networks with varying configurations.
- Investigation of Primary Frequency Control: Assessment of the primary frequency control response in multi-area power systems with different structural arrangements.

2. LOAD FREQUENCY CONTROL

Hierarchical control, as illustrated in Fig. 1, represents a widely adopted approach for mitigating frequency oscillations in power systems. Such control architectures are typically organized into three distinct layers: primary, secondary, and tertiary control. However, depending on the operational circumstances, the magnitude of disturbances, and the extent of frequency deviations, it may be necessary to implement an emergency control loop to restore system frequency and ensure stability rapidly.

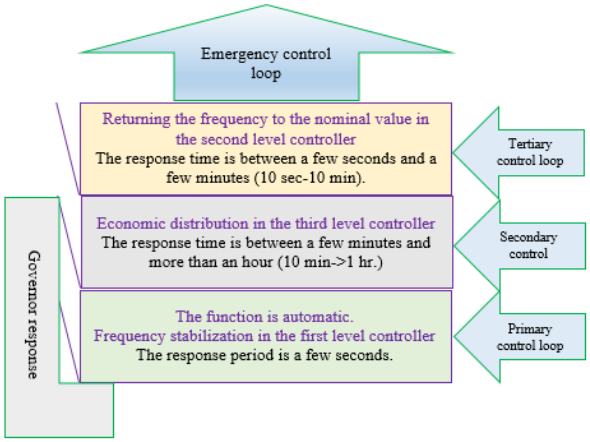

Fig. 1 – Frequency control loops in the power system.

The primary control loop typically mitigates minor frequency fluctuations occurring during regular power system operation. The secondary control loop is activated in response to abnormal conditions, utilizing available stored energy to restore the system frequency. In cases of large disturbances that result in a significant imbalance between generation and load demand, the tertiary control loop is employed to limit frequency deviations and stabilize the system [22].

3. INTERCONNECTED POWER SYSTEM MODEL

Figure 2 shows the connection between one area and other areas in an interconnected power system, where T_{ij} is the synchronizing torque coefficient of the tie-line between two areas i and j. ΔP_d is the incremental changes in load demand, Δf is the incremental changes in system frequency, and ΔP_m is the incremental changes in mechanical power. The error signal of the incremental changes in the connection line power is considered based on the frequency difference between the areas [23,24]. The linearized equations representing the dynamic model of each power plant are described below. Each area has two input signals including u_1=load demand changes (ΔP_d) and u_2=load reference set-point. ΔP_{tie} is the tie-line power flows throughout the tie-line between existing areas. The order of the system matrix (number of state variables) for describing the power plant model in state space is 4, 4, 5, and 3 for steam power plant with reheater, hydro power plant, gas power plant, and steam power plant without reheater, respectively.

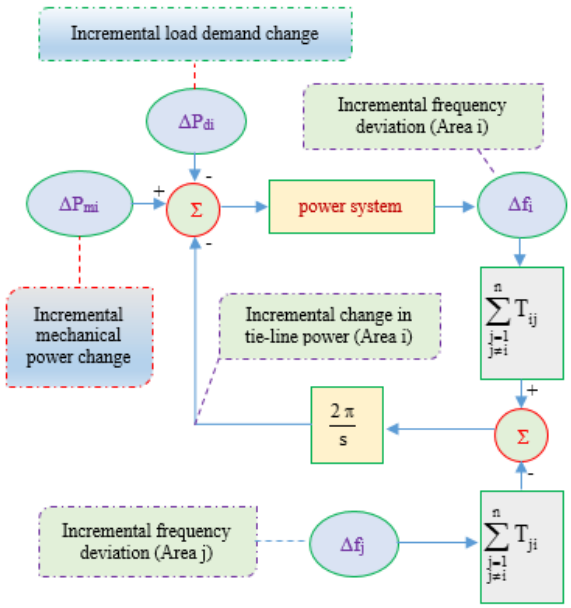

Fig. 2 – Connection between adjacent areas in the interconnected power system.

3.1 SMALL SIGNAL MODEL EQUATIONS OF A STEAM POWER PLANT WITH A REHEATER IN STATE SPACE

By choosing four state variables, x_1=frequency changes (Δf), x_2=turbine output mechanical power changes (ΔP_m), x_3=turbine output mechanical power changes without reheater, and x_4=steam valve changes, the first order differential equations representing the dynamic model of a steam power plant with reheater are expressed as follows.

$$\frac{d}{dt}x_1 = -\frac{K_D}{J_M}x_1 + \frac{1}{J_M}x_2 \pm \frac{1}{J_M}\sum \Delta P_{tie} - \frac{1}{J_M}u_1. \quad (1)$$

$$\frac{d}{dt}x_2 = -\frac{1}{T_H}x_2 + (\frac{1}{T_H} - \frac{F_H}{T_T})x_3 + \frac{F_H}{T_T}x_4. \quad (2)$$

$$\frac{d}{dt}x_3 = -\frac{1}{T_T}x_3 + \frac{1}{T_T}x_4. \quad (3)$$

$$\frac{d}{dt}x_4 = -\frac{K_G}{T_G R_S}x_1 - \frac{1}{T_G}x_4 + \frac{K_G}{T_G}u_2. \quad (4)$$

where T_H is time constant of reheater, F_H is fraction of power generated by high pressure section, T_T is time constant turbine, R_S is speed governor regulation and T_G is speed governor time constant.

3.2 SMALL SIGNAL MODEL EQUATIONS OF HYDROPOWER IN STATE SPACE

To express the first-order differential equations representing the dynamic model of the hydropower plant, four state variables are used, including x_1 frequency changes (Δf), x_2 turbine output mechanical power changes (ΔP_m), x_3 transformer droop compensation output, and x_4 water valve changes.

$$\frac{d}{dt}x_1 = -\frac{K_D}{J_M}x_1 + \frac{K_1}{J_M}x_2 \pm \frac{1}{J_M}\sum \Delta P_{tie} - \frac{1}{J_M}u_1. \quad (5)$$

$$\frac{d}{dt}x_2 == \frac{2T_R K_G}{R_H T_P T_G}x_1 - \frac{2}{T_W}x_2 + (\frac{2}{T_W} + \frac{2}{T_P})x_3 - (\frac{2}{T_P} - \frac{2T_R}{T_P T_G})x_4 - \frac{2K_G T_R}{T_P T_G}u_2. \quad (6)$$

$$\frac{d}{dt}x_3 = -\frac{K_G T_R}{R_H T_G T_P}x_1 - \frac{1}{T_P}x_3 + (\frac{1}{T_P} - \frac{T_R}{T_P T_G})x_4 + \frac{K_G T_R}{T_G T_P}u_2. \quad (7)$$

$$\frac{d}{dt}x_4 = -\frac{K_G}{R_H T_G}x_1 - \frac{1}{T_G}x_4 + \frac{K_G}{T_G}u_2. \quad (8)$$

where J_M is equivalent inertia constant, K_D is equivalent damping factor of the loads, T_W is water starting time, T_R is speed governor reset time, T_P is transient droop time constant, R_H is speed governor regulation and T_G is main server time constant.

3.3 SMALL SIGNAL MODEL EQUATIONS OF GAS POWER PLANT IN STATE SPACE

To display the first order differential equations in order to display the small signal model of the gas power plant, five state variables are used, which are: x_1=frequency changes (Δf), x_2= compressor output power changes, x_3=.fuel system output power changes, x_4= speed governor output power changes and x_5= valve position output power changes.

$$\frac{d}{dt}x_1 = -\frac{K_D}{J_M}x_1 + \frac{1}{J_M}x_2 \pm \frac{1}{J_M}\sum \Delta P_{tie} - \frac{1}{J_M}u_1. \quad (9)$$

$$\frac{d}{dt}x_2 = -\frac{1}{T_D}x_2 + \frac{1}{T_D}x_3. \quad (10)$$

$$\frac{d}{dt}x_3 = \frac{T_{CR}K_V T_L}{T_V T_F R_G T_G}x_1 - \frac{1}{T_F}x_3 + \frac{1}{T_F}(\frac{T_{CR}}{T_G} + 1)x_4 + \frac{T_{CR}}{T_G T_F}(\frac{T_L}{T_V} - 1)x_5 - \frac{T_{CR}K_V T_L}{T_F T_V T_G}u_2. \quad (11)$$

$$\frac{d}{dt}x_4 = -\frac{K_V T_L}{T_V R_G T_G}x_1 - \frac{1}{T_G}x_4 - \frac{1}{T_G}(\frac{T_L}{T_V} - 1)x_5 + \frac{K_V T_L}{T_V T_G}u_2 \quad (12)$$

$$\frac{d}{dt}x_5 = -\frac{K_V}{T_V R_G}x_1 - \frac{1}{T_V}x_5 + \frac{K_V}{T_V}u_2. \quad (13)$$

where T_G Is time constant of the speed governor lag, T_L is time constant of the speed governor lead, R_G is speed governor regulation, T_F is fuel time constant, T_{CR} is time delays of the combustion reaction, T_{CD} is time constant of the compressor discharge volume, K_V is value positioner gain and T_V is time constant of the value positioner. Fig. 3 shows the connection of three different areas. The output signal in each area is considered to be the frequency deviation of the same area [25]. Therefore, according to the power change of the connecting line between the areas, the number of state variables to display the connected power system, two-area or three-area, will be at least 8 and at most 16.

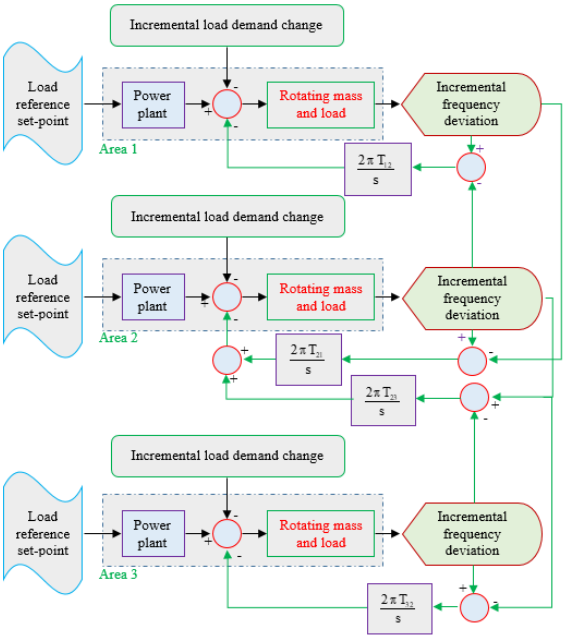

Fig. 3 – Block diagram of a three-area interconnected power system.

4. SIMULATION RESULTS AND DISCUSSION

Controlling the stability of frequency and terminal voltage at nominal values is always essential for good operation of an interconnected power system. In this section, the dynamic behavior of the load frequency control system in the interconnected power system with different combinations of power plants is simulated. The modes of the system are determined for each scenario, and the correctness of the simulation results in the time domain is shown based on them. The parameters of the studied power system are given in Table 1.

Table 1

Plant parameters for simulation.

Parameter	Value
Parameters for hydro power plant	J_M=8, K_D=1, T_W=1, T_R=6, T_P=9.5, R_H=0.1, T_G=0.2
Parameters for steam power plant	J_M=8, K_D=1, T_H=8, F_H=0.4, T_T=0.3, R_S=0.2, T_G=0.3
Parameters for gas power plant	J_M=8, K_D=1, T_G=1.1, T_L=0.6, R_G=0.2, T_P=0.239, T_{CR}=0.01, T_{CD}=0.3, K_V=1, T_V=0.049

4.1 SINGLE-AREA POWER SYSTEM (AREAS INDEPENDENT FUNCTION)

First, in this section, the frequency changes in each of the power plants are examined independently for step changes in load. Figs. 4 and 5 show the transient response of frequency changes in each generation unit. The system modes for each generation unit in this scenario are given in Table 2.

Considering the location of the system modes on the left side of the imaginary axis, as seen in the simulation results, the response will be stable. Table 3 shows the maximum frequency drop and its occurrence time for each generation unit for step changes in load. The lowest frequency drop occurred in the gas unit and the maximum frequency drop occurred in the hydro unit. Also, in terms of response speed, the gas unit operates faster than the other two generation units. The frequency drop in the steam unit is less than the other two units, and for this reason, the mechanical power generation in the steam unit will be greater than the other two units. The steady state frequency in each generating unit depends on the equivalent damping factor of the loads and the speed governor regulation. Since these values are assumed to be the same in all three generating units, the final frequency value will be the same in all three generating units.

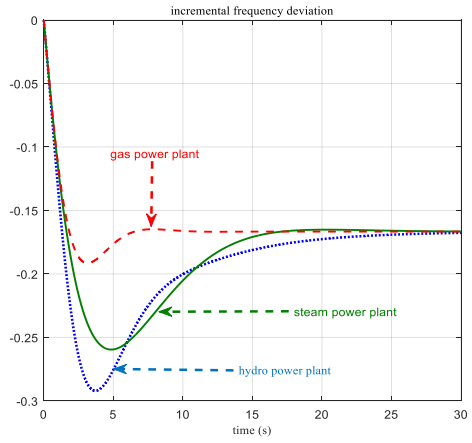

Fig. 4 – Area frequency deviation after step load perturbation in scenario 1 (areas independent function)

Table 2

Power system modes of each area in separate operation

Power plant	Eigenvalues in each area
Steam power plant	-4.1450, -2.2391, -0.2663±j0.2033
Hydro power plant	-5.9738, -0.1773, -0.5308±j0.5826
Gas power plant	-20.3881, -4.8966, -2.5665, -0.5542±j0.6710

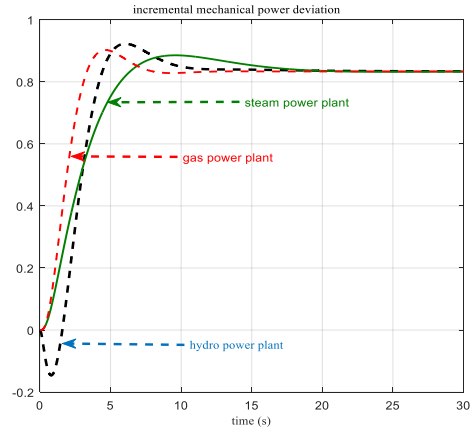

Fig. 5 – Incremental changes in the output mechanical power of turbine after step load perturbation in scenario 1 (areas independent function).

Table 3

The amount of maximum frequency droop for step changes in demand load

Power plant	Maximum frequency drop	Occurrence time
Steam power plant	-0.2596	4.8506
Hydro power plant	-0.2908	3.5935
Gas power plant	-0.1915	3.1482

4.2 TWO-AREA POWER SYSTEM (STEAM POWER PLANT AND HYDRO POWER PLANT)

The dynamic behavior of a two-area power system consisting of two steam and hydro units is simulated in this section. The load step changes in each area are considered separately, and the frequency changes of the steam generation unit (area 1) and the hydro generation unit (area 2) are shown in Figs. 6 and 7, respectively.

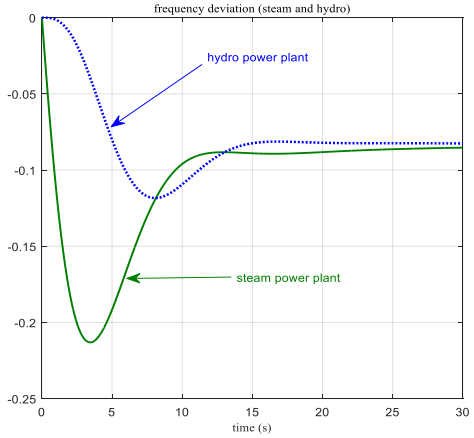

Fig. 6 – Area frequency deviation after step load perturbation in area 1 (steam power plant) in scenario 2.

The system in this case will have two oscillation modes -0.3648±j 0.5575 and -0.3526±j0.3709. The frequency in each zone decreases to -0825 in the steady state. The mechanical power variations for the two generating units for step changes in load in area 2 are shown in Fig. 8. As can be seen, the steam generating unit has less fluctuations than the hydro generating unit. The system in this scenario also has five real modes, which are: -5.9723, -4.1435, -2.2491, -0.2540, and -0.0757.

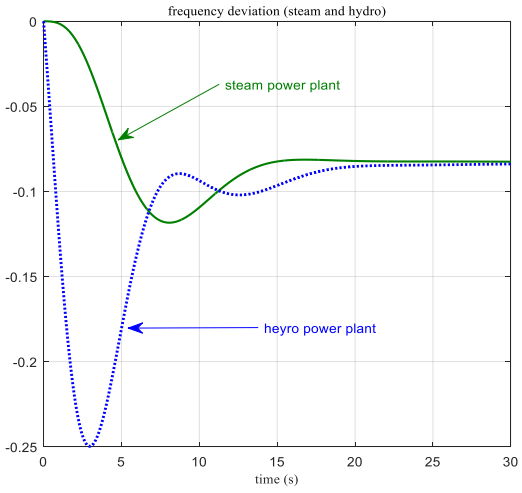

Fig. 7 – Area frequency deviation after step load perturbation in area 2 (hydro power plant) in scenario 2

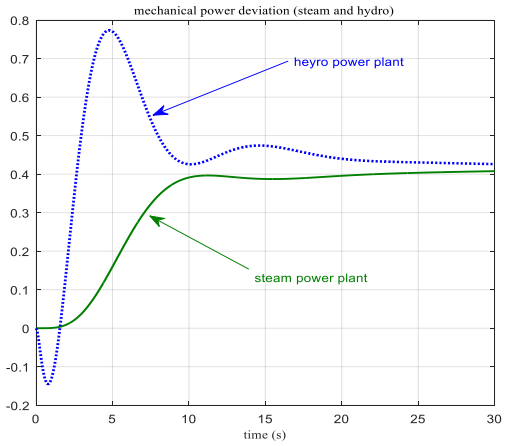

Fig. 8 – Mechanical power deviation after step load perturbation in area 2 (hydro power plant) in scenario 2.

4.3 TWO-AREA POWER SYSTEM (STEAM POWER PLANT AND GAS POWER PLANT)

Steam and gas power plants are common power plants for generating electricity in the power system. The system studied in this section is a two-zone power system including these two generating units. Figure 9 shows the frequency changes in each generating unit for step changes in load in zone 2. As can be seen, the frequency has decreased by 0.0829. The mechanical power output of each generating unit in the steady state is 0.4176 per unit, and the inter-zone power is 0.5 per unit. When the load changes occur in zone 1, the frequency drops to 0.0833. As is clear from the simulation results, when the load changes occur in zone 2, that is, in a gas power plant or a hydro power plant, the frequency drop in zone 1, that is, a steam power plant, will be greater.

Therefore, for supplying the load during the maximum consumption, the gas power plant is very suitable, but the steam power plant is not suitable for supplying the load during the maximum consumption.

As can be seen, in the gas power plant, the maximum frequency drop of 0.1722 Hz occurs at 2.5958 seconds, but in the steam power plant, the maximum frequency drop of 0.0890 Hz occurs at 9.1680 seconds.

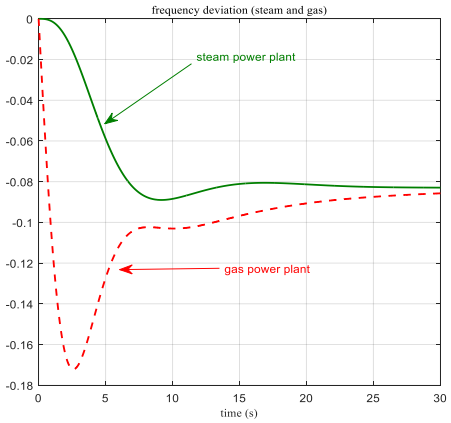

Fig. 9 – Area frequency deviation after step load perturbation in area 2 (gas power plant) in scenario 3.

4.4 THREE-AREA INTERCONNECTED POWER SYSTEM

In this section, a three-zone power system is considered, comprising three generating units: a hydro unit (zone 1), a steam unit (zone 2), and a gas unit (zone 3). The load changes in each zone are considered separately, and the simulation results of the frequency changes of different zones are shown in Figures 10, 11, and 12 for each case. As can be seen, the frequency drop in different cases is 0.0584, 0.0543, and 0.0020. The eigenvalues of the system matrix are given in Table 4.

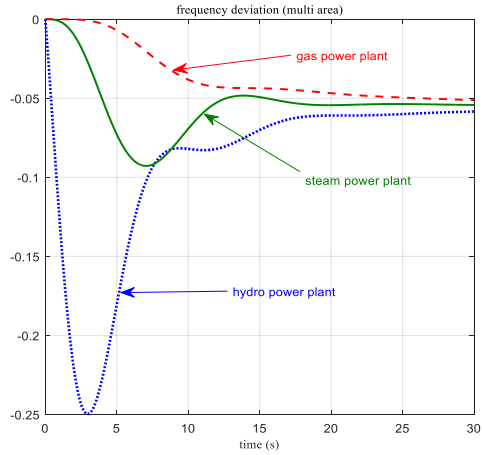

Fig. 10 – Area frequency deviation after step load perturbation in area 1 (steam power plant) in scenario 4.

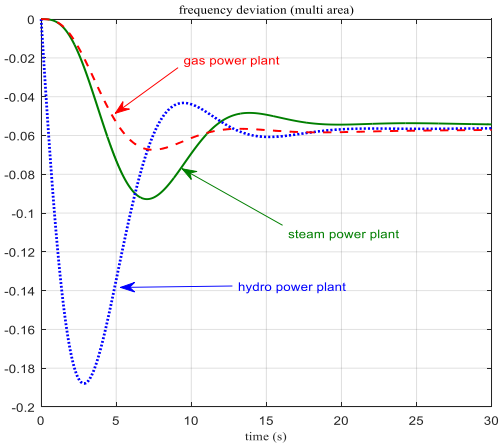

Fig. 11- Area frequency deviation after step load perturbation in area 2 (steam power plant) in scenario 4

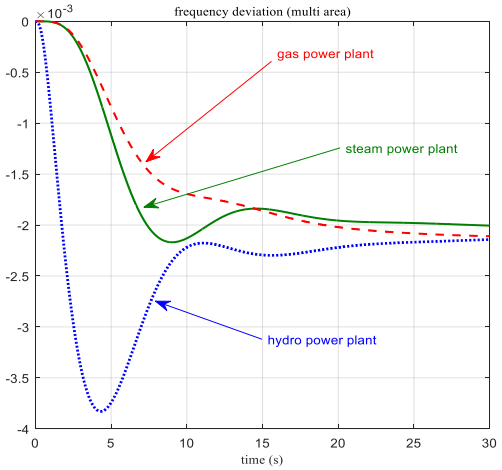

Fig. 12 – Area frequency deviation after step load perturbation in area 3 (steam power plant) in scenario 4.

As can be seen, the eigenvalues are located on the left side of the imaginary axis, which indicates the stability of the power system for small changes in the demand load.

Table 4
Eigenvalues of the system matrix in the interconnected power system for different scenarios

Combination of areas	Eigenvalues in interconnected power system
Steam + Hydro	-0.0528, -0.3021, -2.2491, -4.1435, -5.9666, -0.3014±j0.5574, -0.3843±j0.3156
Steam + Gas	-0.1113, -2.2488, -2.5717, -4.1435, -4.8953, -20.3881, -0.4976±j0.6857, -0.2612±j0.3520
Steam +Hydro + Gas	-0.0388, -0.1117, -0.3697, -2.2584, -2.5717, -4.1420, -4.8953, -5.9666, -20.3881, -0.4987±j0.6847, -0.3823±j0.4124, -0.2705±j0.5744

5. CONCLUSIONS

The expansion of power system capacity alongside the integration of diverse energy sources has significantly increased the complexity of modern electrical grids, leading to inherently nonlinear system behavior. This nonlinear and intricate nature introduces numerous challenges, among which frequency deviation stands out as a critical issue. Maintaining both frequency and voltage within their prescribed standard limits during system operation is essential to ensure the high quality and reliability of the electrical power supply. Interconnected power systems offer several benefits, including the ability to balance discrepancies between supply and demand, facilitate the integration of intermittent renewable energy sources, and enable access to geographically distant energy resources. However, a notable drawback of such interconnected networks is the potential for fault propagation across the entire system, which can jeopardize overall system stability. Therefore, effective management strategies are essential for maintaining the reliability of interconnected systems.

In this paper, the analysis and simulation of the dynamic behavior of the load frequency control system in the time domain for an interconnected power system are presented. The dynamic behavior of the power system is investigated using the analysis of multi-zone power system modes, including various combinations of steam, gas, and hydroelectric power plants. The consumption of active power and reactive power is affected by load changes or any other disturbances, which can severely impact the regular operation of the interconnected power system. To maintain the frequency at the nominal value, a frequency load control system is installed in the generating station, ensuring that with changes in the active power demand, the system frequency and the power passing through the connection lines remain within the specified limits. Due to their quick response, gas turbine units can provide flexible tuning capabilities for power systems.

Received on 4 December 2024

REFERENCES

1. G. Shahgholian, M. R. Moradian, A. Fathollahi, *Droop control strategy in inverter-based microgrids: A brief review on analysis and application in islanded mode of operation*, IET Renewable Power Generation, **19**, *1*(2025).
2. M. Gholami, M. Mallaki, *Increase flexibility and improve resilience in smart microgrids by coordinating storage resources and distributed generation during contingencies*, Journal of Southern Communication Engineering, **12**, *45*, pp. 45–60 (2022).
3. P. Casati, M. Moner-Girona, S.I. Khaleel, S. Szabo, G. Nhamo, *Clean energy access as an enabler for social development: A multidimensional analysis for Sub-Saharan Africa*, Energy for Sustainable Development, **72**, pp. 114–126 (2023).
4. S.A. Rasaki, C. Liu, C. Lao, H. Zhang, Z. Chen, *The innovative contribution of additive manufacturing towards revolutionizing fuel cell fabrication for clean energy generation: A comprehensive review*, Renewable and Sustainable Energy Reviews, **148**, Article Number: 111369 (2021).
5. G. Shahgholian, S.M.A. Zanjani, *A study of voltage sag in distribution system and evaluation of the effect of wind farm equipped with doubly-fed induction generator*, Revue Roumaine des Sciences Techniques, **68**, *3*, pp. 271–276 (2023).
6. Y. Jin, P. Behrens, A. Tukker, L. Scherer, *Water use of electricity technologies: A global meta-analysis*. Renewable and Sustainable Energy Reviews, **115**, Article Number: 109391 (2019).
7. M. Babaei, M. Jahangiri, F. Raeiszadeh, G. R. Aboutalebi, A. Jafari, A. Nariman, *The feasibility of using solar heating in the Yazd hospital: A case study*, Journal of Simulation and Analysis of Novel Technologies in Mechanical Engineering, **15**, *2*, pp. 17–28 (2023).
8. S.A. Ardeh, M. Tabrizian, H. Shahmirzad, *Coordinated operation of gas-electricity integrated distribution network with CCHP and renewable energy sources*, Journal of Novel Researches on Smart Power Systems, **11**, *3*, pp. 43–53 (2022).
9. M.J.B. Kabeyi, O.A. Olanrewaju, *The levelized cost of energy and modifications for use in electricity generation planning*, Energy Reports, **9**, *9*, pp. 495–534 (2023).
10. A. Boulayoune, A. Oubelaid, A. Chibah, *Comparative study of inner and outer rotor flux reversal permanent magnet machine for direct drive wind turbine*, Revue Roumaine des Sciences Techniques, **69**, *2* (2024).
11. W. Srisuwan, W. Sa-Ngiamvibool, *Optimal controller design for isolated hybrid wind-diesel power system using bee algorithm*, Revue Roumaine des Sciences Techniques, **64**, *4*, pp. 341–348 (2019).
12. B. Li, S. Hu, Q. Zhong, K. Shi, S. Zhong, *Dynamic memory event-triggered proportional-integral-based H∞ load frequency control for multi-area wind power systems*, Applied Mathematics and Computation, **453**, Article Number: 128070 (2023).
13. H. Erol, S. Ayasun, *Gain-phase margins-based stability analysis of time delayed hybrid load frequency control system*, Revue Roumaine des Sciences Techniques, **66**, *2*, pp. 119–124 (2021).
14. Y. Jia, Z. Y. Dong, C. Sun, K. Meng, *Cooperation-based distributed economic MPC for economic load dispatch and load frequency control of interconnected power systems*, IEEE Transactions on Power Systems, **34**, *5*, pp. 3964–3966 (2019).
15. T. Ali, S.A. Malik, I.A. Hameed, A. Daraz, H. Mujlid, A.T. Azar, *Load frequency control and automatic voltage regulation in a multi-area interconnected power system using nature-inspired computation-based control methodology*, Sustainability, **14**, Article Number: 12162 (2022).
16. A.O. Aluko, R. Carpanen, D.G. Dorrell, E.E. Ojo, *Robust state estimation method for adaptive load frequency control of interconnected power system in a restructured environment*, IEEE Systems Journal, **15**, *4*, pp. 5046–5056 (2021).
17. R. Rajan, F.M. Fernandez, *Small-signal stability analysis and frequency regulation strategy for photovoltaic sources in interconnected power systems*, Electrical Engineering, **103**, pp. 3005–3021 (2021).
18. G. Q. Zeng, X.Q. Xie, M.R. Chen, *An adaptive model predictive load frequency control method for multi-area interconnected power systems with photovoltaic generations*, Energies, **10**, Article Number: 1840 (2017).
19. M. Yang, W. Chunsheng, H. Yukun, L. Zijian, Y. Caixin, H. Shuhang, *Load frequency control of photovoltaic generation-integrated multi-area interconnected power systems based on double equivalent-input-disturbance controllers*, Energies, **13**, *22*, Article Number: 6103 (2020).
20. N. Hakimuddin, I. Nasiruddin, T.S. Bhatti, Y. Arya, *Optimal automatic generation control with hydro, thermal, gas, and wind power plants in a 2-area interconnected power system*, Electric Power Components and Systems, **48**, *6–7*, pp. 558–571 (2020).
21. Y. Zheng, J. Tao, Q. Sun, H. Sun, Z. Chen, M. Sun, *Deep reinforcement learning based active disturbance rejection load frequency control of multi-area interconnected power systems with renewable energy*, Journal of Franklin Institute, **360**, *17*, pp. 13908–13931 (2023).
22. B.M. Patre, P.S. Londhe, R.M. Nagarale, *Fuzzy sliding mode control for spatial control of large nuclear reactor*, IEEE Transactions on Nuclear Science, **62**, *5*, pp. 2255–2265 (2015).
23. C.N.S. Kalyan, C.V. Suresh, *Higher order degree of freedom controller for load frequency control of multi-area interconnected power system with time delays*, Global Transitions Proceedings, **3**, *1*, pp. 332–337 (2022).
24. F. Zhu, X. Zhou, Y. Zhang, D. Xu, J. Fu, *A load frequency control strategy based on disturbance reconstruction for multi-area interconnected power system with hybrid energy storage system*, Energy Reports, **7**, pp. 8849–8857 (2021).
25. G. Chen, Z. Li, Z. Zhang, S. Li, *An improved ACO algorithm optimized fuzzy PID controller for load frequency control in multi area interconnected power systems*, IEEE Access, **8**, pp. 6429–6447 (2020).